

**MESOPOROUS MCM-41, MCM-48, SBA-15, AND PYROLYSIS CHAR AS
CATALYSTS FOR CATALYTIC PYROLYSIS OF WASTE TIRE**

Supattra Seng-eiad

A Thesis Submitted in Partial Fulfillment of the Requirements
for the Degree of Master of Science
The Petroleum and Petrochemical College, Chulalongkorn University
in Academic Partnership with
The University of Michigan, The University of Oklahoma,
Case Western Reserve University, and Institut Français du Pétrole
2015


I 28368 344

Thesis Title: Mesoporous MCM-41, MCM-48, SBA-15, and Pyrolysis
Char as Catalysts for Catalytic Pyrolysis of Waste Tire
By: Ms. Supattra Seng-eiad
Program: Petrochemical Technology
Thesis Advisor: Assoc. Prof. Sirirat Jitkarnka

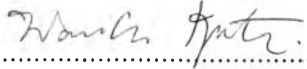
Accepted by The Petroleum and Petrochemical College, Chulalongkorn
University, in partial fulfillment of the requirements for the Degree of Master of
Science.


..... College Dean
(Asst. Prof. Pomthong Malakul)

Thesis Committee:


.....
(Assoc. Prof. Sirirat Jitkarnka)


.....
(Assoc. Prof. Apanee Luengnaruemichai)


.....
(Asst. Prof. Wanida Koo-amornpattra)

ABSTRACT

5671034063: Petrochemical Technology Program
Supattra Seng-eiad: Mesoporous MCM-41, MCM-48, SBA-15, and
Pyrolysis Char as Catalysts for Catalytic Pyrolysis of Waste Tire.
Thesis Advisor: Assoc. Prof. Sirirat Jitkarnka 204 pp.
Keywords: Molecular diameters/ Catalysts design/ Mesoporous materials/
Pyrolysis char/ Nitrogenous compound identification/
Petrochemicals/ Sulfur removal/ Waste tire pyrolysis

Due to the fact that aromatic compounds and hetero-atoms such as nitrogen are present, tire-derived oil (TDO) is not suitable for direct uses in a vehicle engine. Additionally, char remaining from pyrolysis is highly obtained, but it has only a few applications. Therefore, the objectives were to (1) design catalysts for removal of heavy compounds in TDO, (2) study the effect of pore size and pore structure of selected catalysts, (3) upgrade pyrolysis char for using as catalyst, and (4) identify N-containing compounds for better understanding in further treatment. The result indicated that aromatic compounds (size 8-16 Å by average) were mainly in gas oil and vacuum gas oil fractions. The selected catalysts, like mesoporous materials, were thus suggested to handle these compounds. Subsequently, mesoporous Al-MCM-41 (33.1 Å) and Al-SBA-15 (60.5 Å) were used to study the effect of pore size whereas mesoporous Si-MCM-41 (hexagonal structure) and Si-MCM-48 (cubic structure) were used to study the effect of pore structure. As a result, the pore size of 33.1 Å and cubic structure gave better removal of heavy compounds, petrochemical productivity, and sulfur removal. Furthermore, pyrolysis chars with and without treatment well performed on improving lighter fractions from conversion of heavy portions. Moreover, identification of nitrogenous compounds in TDO was successfully accomplished using an effective GCxGC/TOF-MS. The detected species were classified into 10 groups. Interestingly, diazabicycloheptenes is a new group, firstly detected in TDO, owing to the high performances of GCxGC/TOF-MS on separation and detection of highly-complex mixtures.

บทคัดย่อ

สุพัตรา เสี่ยงเอียด : การใช้วัสดุที่มีรูพรุนขนาดกลางเอ็มซีเอ็ม-41, เอ็มซีเอ็ม-48, เอสบีเอ-15, และไพโรไลซิสชาร์เป็นตัวเร่งปฏิกิริยาสำหรับกระบวนการไพโรไลซิสของหมวดสภาพ (Mesoporous MCM-41, MCM-48, SBA-15, and Pyrolysis Char as Catalysts for Catalytic Pyrolysis of Waste Tire) อ. ที่ปรึกษา : รศ. ดร. ศิริรัตน์ จิตการคำ 204 หน้า

ด้วยเหตุผลที่ว่าสารประกอบแอโรเมติกส์และวิวิธพันธ์อะตอม เช่น ไนโตรเจน เป็นองค์ประกอบในน้ำมัน ดังนั้นน้ำมันที่ได้จากกระบวนการไพโรไลซิสจึงยังไม่เหมาะต่อการนำไปใช้โดยตรงกับยานยนต์ ยิ่งไปกว่านั้นกระบวนการไพโรไลซิสยังสามารถผลิตชาร์ได้ในปริมาณมากแต่มีการนำไปประยุกต์ใช้น้อย ดังนั้นจุดประสงค์ของงานนี้คือเพื่อที่จะ (1) ออกแบบตัวเร่งปฏิกิริยาสำหรับการกำจัดสารไฮโดรคาร์บอนหนัก, (2) เพื่อที่จะศึกษาอิทธิพลของขนาดรูพรุนและโครงสร้างของตัวเร่งปฏิกิริยาที่ถูกเลือกมาใช้, (3) เพื่อที่จะเพิ่มคุณสมบัติของไพโรไลซิสชาร์สำหรับใช้เป็นตัวเร่งปฏิกิริยา และ (4) เพื่อที่จะระบุพารามิเตอร์ประกอบไนโตรเจนเพื่อสร้างความเข้าใจที่มากขึ้นในการปรับปรุงคุณภาพต่อไป จากผลการทดลองแสดงให้เห็นว่าสารประกอบแอโรเมติกส์ (ขนาด 8-16 อังสตรอม โดยเฉลี่ย) เป็นองค์ประกอบหลักในน้ำมันเตาและน้ำมันเตาสุญญากาศ ดังนั้นตัวเร่งปฏิกิริยา เช่น วัสดุที่มีรูพรุนขนาดกลางจึงถูกแนะนำเพื่อใช้จัดการกับสารประกอบเหล่านี้ หลังจากนั้นวัสดุที่มีรูพรุนขนาดกลางอลูมินาเอ็มซีเอ็ม-41 (รูพรุน 33.1 อังสตรอม) และอลูมินาเอสบีเอ-15 (รูพรุน 60.5 อังสตรอม) จึงถูกนำมาศึกษาอิทธิพลของขนาดรูพรุน ในขณะที่ซิลิกาเอ็มซีเอ็ม-41 (โครงสร้างแบบหกเหลี่ยม) และ ซิลิกาเอ็มซีเอ็ม-48 (โครงสร้างแบบลูกบาศก์) ถูกนำมาศึกษาอิทธิพลของโครงสร้าง ผลลัพธ์ที่ได้พบว่า รูพรุนขนาด 33.1 อังสตรอม และ โครงสร้างแบบลูกบาศก์ สามารถใช้กำจัดสารไฮโดรคาร์บอนหนัก เพิ่มผลผลิตปิโตรเคมีและกำจัดซัลเฟอร์ได้ดีกว่า นอกจากนี้ไพโรไลซิสชาร์ทั้งที่บำบัดและไม่บำบัดยังมีประสิทธิภาพในการปรับปรุงสารประกอบเบาจากการเปลี่ยนแปลงของสารประกอบหลักได้เป็นอย่างดี นอกจากนี้ยังประสบความสำเร็จในการระบุพารามิเตอร์ของสารประกอบไนโตรเจนที่มีอยู่ในน้ำมันโดยใช้ GCxGC/TOF-MS โดยสารประกอบที่ถูกตรวจจับได้ถูกแบ่งออกเป็น 10 กลุ่ม สิ่งที่น่าสนใจก็คือ ไดอะซาไบไซโคลเฮปทีนส์ เป็นไนโตรเจนกลุ่มใหม่ที่สามารถตรวจวัดได้ครั้งแรกในน้ำมันที่ได้จากกระบวนการไพโรไลซิส อันเนื่องมาจากความมีประสิทธิภาพสูงของ GCxGC/TOF-MS ในการแยกและตรวจวัดสารที่มีองค์ประกอบซับซ้อนมากๆ ได้

ACKNOWLEDGEMENTS

This thesis work would not have been accomplished without these following people whom I am gratefully indebted for individual and organization.

I would like to express my deepest appreciation to my supervisor, Assoc. Prof. Sirirat Jitkarnka who is beyond an advisor. I was supported by her in every single thing including excellent guideline, useful recommendations, creative comment, intensive attention, and encouragement throughout the year of research. She has not only taught me about the theoretical knowledge but also made me realize in myself. I feel proud to be her junior student.

I would like to give special thanks to the thesis committee, Assoc. Prof. Apanee Luengnaruemichai and Asst. Prof. Wanida Koo-amornpattra for giving valuable guidelines and suggestions.

This research work was partially supported by the Ratchadapisek Sompoch Endowment Fund (2013), Chulalongkorn University (CU-56-900-FC) and Thailand Research Fund (IRG5780012).

Moreover, the authors would like to thank The Petroleum and Petrochemical College, Chulalongkorn University, Thailand, Center of Excellence on Petrochemical and Materials Technology, and Thailand Research Fund (TRF: RSA5680021) for all supports.

Sincerely, I greatly appreciate all of PPC staff, friends, and SJ- senior students who gave me kind help and morale.

I cannot finish without saying how grateful I am with my family for their unconditional love, support, cheering me up, and all understandings. Without them, I would never have succeeded at this point.

TABLE OF CONTENTS

	PAGE
Title Page	i
Acceptance Page	ii
Abstract (in English)	iii
Abstract (in Thai)	iv
Acknowledgements	v
Table of Contents	vi
List of Tables	xi
List of Figures	xiv
 CHAPTER	
I INTRODUCTION	1
 II THEORETICAL BACKGROUND AND LITERATURE REVIEW	
	4
2.1 Drawbacks of Pyrolysis Products	4
2.2 Catalyst Design	7
2.3 Mesoporous Materials	8
2.3.1 Meso-silica Materials	9
2.3.2 Pyrolysis Char	17
2.4 Catalytic Mechanism	20
2.5 Identification of Nitrogenous Compounds in Tire-derived Oil	22
2.6 Research Motivation	24
2.7 Objectives and Scopes of Research Work	26
 III EXPERIMENTAL	
	29
3.1 Materials and Equipments	29

CHAPTER	PAGE
3.1.1 Materials	29
3.1.2 Equipments	29
3.2 Chemicals and Solvents	30
3.3 Experimental Procedures	30
3.3.1 Catalyst Preparation	30
3.3.2 Catalyst Characterization	33
3.3.3 Pyrolysis Process	35
3.3.4 Product Analysis	36
IV ESTIMATION OF AVERAGE KINETIC AND MAXIMUM DIAMETERS OF HYDROCARBON GROUPS IN TIRE-DERIVED OIL FOR CATALYST DESIGN PURPOSE	43
4.1 Abstract	43
4.2 Introduction	43
4.3 Experimental	45
4.3.1 Pyrolysis Process of Waste Tire	45
4.3.2 Analysis of Waste Tire Products	45
4.3.3 Determination of Sampling Size	46
4.3.4 Determination of Molecular Diameters	46
4.4 Results and Discussion	48
4.4.1 Analysis of Tire-derived Oil	48
4.4.2 Determination of Sampling Size	49
4.4.3 Determination of Molecular Diameters	50
4.4.4 Design of Catalyst	51
4.5 Conclusions	54
4.6 Acknowledgements	55
4.7 References	55

CHAPTER	PAGE
V	
REMOVAL OF AROMATIC MOLECULES AND SULFUR COMPOUNDS IN TIRE-DERIVED OIL USING MESOPOROUS Al-MCM-41 AND Al-SBA-15 WITH DIFFERENT PORE SIZE	57
5.1 Abstract	57
5.2 Introduction	58
5.3 Experimental	60
5.3.1 Catalyst Preparation	60
5.3.2 Catalyst Characterization	60
5.3.3 Pyrolysis of Waste Tire	61
5.3.4 Product Analysis	61
5.3.5 Determination of Average Maximum Diameters of Molecules in TDOs	63
5.4 Results and Discussion	63
5.4.1 Catalyst Characterization	63
5.4.2 Product from Waste Tire Pyrolysis	65
5.4.3 Molecular Size Distribution of Aromatic Compounds in Tire-derived Oil	68
5.4.4 Petrochemical Productivity using Mesoporous Al-MCM-41 and Al-SBA-15	73
5.4.5 Hetero-atom Removal Using Mesoporous Al-MCM-41 and Al-SBA-15	74
5.5 Conclusions	75
5.6 Acknowledgements	75
5.7 References	76

CHAPTER		PAGE
VI	SYNTHESIS OF MESOPOROUS Si-MCM-41 AND Si-MCM-48 AT ROOM TEMPERATURE AND THEIR CATALYTIC ACTIVITY IN WASTE TIRE PYROLYSIS: EFFECTS OF PORE STRUCTURE	75
	6.1 Abstract	75
	6.2 Introduction	79
	6.3 Experimental	80
	6.3.1 Synthesis of Si-MCM-41 and Si-MCM-48	80
	6.3.2 Catalyst Characterization	81
	6.3.3 Pyrolysis of Waste Tire	82
	6.3.4 Product Analysis	82
	6.3.5 Determination of Sampling Size	83
	6.4 Results and Discussion	84
	6.4.1 Catalyst Characterization	84
	6.4.2 Effect of Pore Structure on Waste Tire Pyrolysis Products	87
	6.4.3 Proposed Schemes of Mono-aromatic Formation	93
	6.4.4 Petrochemical Productivity	97
	6.5 Conclusions	99
	6.6 Acknowledgements	100
	6.7 References	100
VII	POSSIBILITY OF USING UNTREATED AND HNO₃-TREATED PYROLYTIC CHAR AS CATALYSTS FOR THERMOLYSIS OF SCRAP RUBBER: IN-DEPTH ANALYSIS OF TIRE-DERIVED PRODUCTS AND CHAR CHARACTERIZATION	103
	7.1 Abstract	103

CHAPTER	PAGE
7.2 Introduction	104
7.3 Experimental	105
7.3.1 Catalyst Preparation	105
7.3.2 Catalyst Characterization	105
7.3.3 Pyrolysis Process	106
7.3.4 Product Analysis	107
7.4 Results and Discussion	107
7.4.1 Characterization of Tire-derived Chars (TDCs)	107
7.4.2 Catalytic Pyrolysis	112
7.4.3 Hetero-atom Removal from Tire-derived Oil	117
7.5 Conclusions	119
7.6 Acknowledgements	119
7.7 References	119
VIII IDENTIFICATION OF NITROGENOUS COMPOUNDS IN TIRE-DERIVED OIL USING POWERFUL GCxGC/TOF-MS FOR BETTER ANALYSIS	122
8.1 Abstract	122
8.2 Introduction	122
8.3 Experimental	125
8.3.1 Pyrolysis of Waste Tire	125
8.3.2 Analysis of Nitrogen Compounds in Tire-derived oil	120
8.4 Results and Discussion	127
8.4.1 Composition of Tire Sample and Pyrolytic Oil	127
8.4.2 Identification of Nitrogenous Compounds in Tire-derived Oil	128

CHAPTER	PAGE
8.4.3 Nitrogenous Compounds in each Petroleum Fractions	148
8.5 Conclusions	149
8.6 Acknowledgements	150
8.7 References	150
IX CONCLUSIONS AND RECOMMENDATIONS	152
REFERENCES	155
APPENDICES	165
Appendix A Estimation of Molecular Size	165
Appendix B Overall Yields of Pyrolysis Products	181
Appendix C Gas Products	182
Appendix D Liquid Products	184
Appendix E Solid Products	195
Appendix F Catalyst Characterizations	203
CURRICULUM VITAE	204

LIST OF TABLES

TABLE	PAGE	
2.1	Elemental composition of pyrolysis carbon	18
3.1	Analysis conditions of GCxGC-TOF/MS	37
3.2	PIANO standard	38
3.2	Analysis conditions of SIMDIST GC	38
3.3	Average peak area of some petrochemical products (BTEXC) in PIANO standard detected from GCxGC/TOF-MS	39
3.4	Analysis conditions of SIMDIST GC	40
3.5	Hydrocarbon ranges divided into the simulating true boiling point by using SIMDIST GC	40
3.6	Analysis conditions of GC/FID	41
3.7	Response factors of gases	42
4.1	Sampling size and representatives from each group of compounds	49
4.2	Average kinetic and maximum diameters of compositions in each group	51
4.3	Molecular composition of each petroleum cuts (%) of thermal pyrolysis case	54
5.1	Porous properties of mesoporous Al-MCM-41 and Al-SBA-15	65
5.2	Ultimate analysis of tire-derived oils	68
5.3	Sampling size and representatives from each molecular group of compounds	69
5.4	Molecular size of dominant aromatic compounds in TDOs from using Al-MCM-41 and Al-SBA-15	70
5.5	Petrochemical productivity using Al-MCM-41 and Al-SBA-15 in waste tire pyrolysis	74

TABLE	PAGE
5.6 Ultimate analysis of hetero-atom (S,N) contents in tire-derived oils	74
6.2 Sampling size and representatives from each molecular group of compounds	91
6.3 Molecular composition of each petroleum cuts (wt%) in maltenes from Si-MCM-41 and Si-MCM-48 cases (1 = Non-catalyst, 2 = Si-MCM-41, and 3 = Si-MCM-48)	92
6.4 Ultimate analysis (wt%) of oil products	93
6.5 Dominant aromatic compounds found in TDOs from using synthesized Si-MCM-41 and Si-MCM-48	94
6.6 Petrochemical productivity from waste tire pyrolysis	98
6.7 Ultimate analysis of hetero-atom (S,N) contents in tire-derived oils	99
7.1 Proximate and ultimate analysis of waste tire sample	108
7.2 Physical properties of untreated char and 5 M HNO ₃ -treated char	109
7.3 Major elements and mineral contents in TDC before and after nitric acid treatment	112
7.4 Element contents in TDO (wt%)	112
8.1 Analysis conditions of GCxGC-TOF/MS	126
8.2 Elemental compositions (wt%) of tire samples and pyrolytic oils	127
8.3 Petroleum fractions of tire-derived oil	128
8.4 Classification of N-containing species based on hydrocarbon groups	129

TABLE	PAGE
8.5 Average normalized nitrogenous composition (%) in tire-derived oil by groups and carbon numbers (An = amines, Ad = amides, Az = azo compounds, DBCH = diazabicycloheptenes, ID = indoles, ITC = isothiocyanates, N = nitro compounds, NT = nitriles, PD = pyridines, and QL = quinolines)	131
8.6 Dominant N-containing compounds in amine group	133
8.7 Dominant N-containing compounds in amide group	125
8.8 Dominant N-containing compounds in azo compound group	137
8.9 Dominant N-containing compounds in diazabicycloheptene group	138
8.10 Dominant N-containing compounds in indole group	140
8.11 Dominant N-containing compounds in isothiocyanate group	141
8.12 Dominant N-containing compounds in nitro compound group	143
8.13 Dominant N-containing compounds in nitrile group	145
8.14 Dominant N-containing compounds in pyridine group	146
8.15 Dominant N-containing compounds in quinoline group	148
A1 Sampling size and representatives from each group of compounds	166
A2 Ranges of molecular size in each hydrocarbon group	168
A3 Concentration of molecules in each hydrocarbon group	168
A4 Average kinetic and maximum diameters of compositions in each group of non-catalyst case	170
B1 Yield of products	181
C1 Yield of gas components	183
D1 Standard (ASTM D2887)	184
D2 Influence of mesoporous materials on boiling point (°C) of maltenes	186

TABLE	PAGE	
D3	Concentration of petroleum fractions in maltenes	187
D4	Concentration of chemical components in maltenes	190
D5	Yield of petrochemicals in maltenes	191
D6	Yield of petrochemicals in mono-aromatics	192
D7	Average peak area of some petrochemical products (BTEXC) in PIANO standard detected from GCxGC/TOF-MS	192
D8	Concentration of petrochemical products in maltenes	193
D9	Influence of mesoporous materials on petroleum fractions (wt%) in maltenes using GCxGC/TOF-MS	194
E1	Total acidity of pyrolysis char	195
E2	Standard of CHNS analysis	196
E3	Calibration of carbon using EDTA standard	196
E4	Calibration of hydrogen using EDTA standard	198
E5	Calibration of nitrogen using EDTA standard	199
E6	Calibration of sulfur using Coal standard	200
E7	Elemental contents (%) in tire-derived oils	201
E8	Sulfur contents in pyrolysis products using mesoporous materials	201
E9	Nitrogen contents in pyrolysis products using mesoporous materials	201
F1	Catalyst properties	203

LIST OF FIGURES

FIGURE	PAGE
2.1	Pyrolysis products. 4
2.2	Classification of hydrocarbons in tire-derived oil. 5
2.3	Classification of mono-aromatic group. 6
2.4	Classification of S-compounds in a tire-derived oil obtained from the non-catalyst batch. 7
2.5	Kinetic and maximum diameters of hydrocarbons. 7
2.6	Different structural types of molecular sieves. 9
2.7	Self-assembly of MCM-41. 10
2.8	Structures of MCM-41, MCM-48, and SBA-15. 11
2.9	Small-angle XRD patterns of (a) MCM-41, (b) MCM-48, and (c) SBA-15. 13
2.10	SEM images of of (a) MCM-41, (b) MCM-48, and (c) SBA-15, and TEM images of of (a) MCM-41, (b) MCM-48, and (c) SBA-15. 13
2.11	Adsorption of sulfur compound on the SBA-15 surface. 16
2.12	Structure of (a) pyrolysis carbon and (b) graphite. 17
2.13	Possible scission position for C-C bonds in the SBR chain during pyrolysis and the resultant resonance aromatic structure for Position (a) . 20
2.14	Energy-minimized structure of the model SBR. 21
2.15	Hydrocarbons interaction with silanol group on MCM-41 surface. 22
2.16	Pore sizes of (a) zeolite and (b) Mesoporous, and the maximum diameter of (c) dibenzylmethane (PAHs) and (d) 1,1'-oxydiethylidene(bis)-benzene (PPAHs). 26
3.1	Synthetic Si-MCM-41 and Si-MCM-48. 31
3.2	Acidic modification of pyrolysis char. 32

FIGURE		PAGE
3.3	Schematic of the pyrolysis process.	36
4.1	(a) Petroleum fractions analyzed by using SIMDIST GC, and (b) maltene compositions of each component group detected by using GCxGC-TOF/MS.	48
4.2	Molecular size distributions of components in: (a) saturated hydrocarbons, (b) olefins, (c) naphthenes, (d) terpenes, (e) mono-aromatics, (f) di-aromatics, (g) poly-aromatics, and (h) polar-aromatics.	50
4.3	(a) Distribution of large-size molecules (T = Tetralines, Akl = Akybenzenes, Ia = Indanes, Ie = Indenes, Ake = Akenylbenzene).	52
4.4	Distribution of molecular sizes of compounds in TDO in all petroleum fractions.	53
5.1	Determination of suitable pore size of mesoporous catalysts for removal of poly- and polar-aromatics in TDOs.	59
5.2	(a) SAXS patterns, (b) FE-SEM image, (c) isotherms, and (d) pore size distributions of Al-MCM-41 and Al-SBA-15.	64
5.3	(a) Product distributions and (b) gas products from using Al- MCM-41 and Al-SBA-15.	65
5.4	Total Ion Chromatograms of maltenes: contour plots (2D) in cases of (a) non-catalyst, (b) Al-MCM-41, and (c) Al-SBA-15, and surface plots (3D) in cases of (d) non-catalyst, (e) Al- MCM-41, and (f) Al-SBA-15.	66
5.5	(a) Chemical compositions and (b) petroleum fractions from using Al-MCM-41 and Al-SBA-15.	67

FIGURE	PAGE
5.6 Molecular size distribution: (a) all groups, (b) polar-aromatics (PPAHs), (c) poly-aromatics (PAHs), (d) di-aromatics (DAHs), and (e) mono-aromatics (MAHs) in maltene obtained from using Al-MCM-41 and Al-SBA-15.	71
5.7 Percentage of petrochemicals in mono-aromatics (B = Benzene, T = Toluene, E = Ethylbenzene, X = Mixed-xylenes, S = Styrene, and C = Cumene).	73
6.1 (a) SAXS patterns, and FE-SEM images of synthetic (b) Si-MCM-41 and (c) Si-MCM-48.	84
6.2 (a) Isotherms, (b) pore size distributions, and (c) TPD-NH ₃ profiles of synthetic Si-MCM-41 and Si-MCM-48.	85
6.3 Silanol groups on the surfaces of mesoporous Si-MCM-41 and Si-MCM-48.	86
6.4 (a) Product distribution, and (b) gas compositions from using synthesized Si-MCM-41 and Si-MCM-48.	88
6.5 Petroleum fraction from using synthesized Si-MCM-41 and Si-MCM-48.	88
6.6 Total Ion Chromatograms of maltenes: contour plots (2D) in cases of (a) non-catalyst, (b) Si-MCM-41, and (c) Si-MCM-48, and surface plots (3D) in cases of (d) non-catalyst, (e) Si-MCM-41, and (f) Si-MCM-48.	89
6.7 Molecular compositions of maltenes from using synthesized Si-MCM-41 and Si-MCM-48.	90
6.8 Proposed reaction schemes for conversion of di-, poly-, and polar-aromatics into mono-aromatics using synthesized mesoporous Si-MCM-41 and Si-MCM-48.	96

FIGURE	PAGE
6.9 Percentage of petrochemicals in mono-aromatic fraction (B = Benzene, T = Toluene, E = Ethylbenzene, X = Mixed-xylenes, S = Styrene, and C = Cumene).	98
7.1 FTIR spectra of untreated and 5 M HNO ₃ -treated char.	109
7.2 (a) Isotherms and (b) pore diameter distributions of untreated and 5 M HNO ₃ -treated char.	110
7.3 XRD patterns of untreated and 5 M HNO ₃ -treated chars (W = wurtzite (α -ZnS), S = sphalerite (β -ZnS))	111
7.4 FE-SEM images of (a) untreated and (b) 5 M HNO ₃ -treated chars.	113
7.5 (a) Product distribution, (b) gas products and (c) petroleum fractions from using pyrolysis char as catalyst.	113
7.6 Total Ion Chromatograms of maltenes: contour plots (2D) in cases of (a) non-catalyst, (b) untreated char, and (c) 5 M HNO ₃ -treated char and surface plots (3D) in cases of (d) non-catalyst, (e) untreated char, and (f) 5 M HNO ₃ -treated char.	115
7.7 Maltene compositions from using pyrolysis chars as catalysts.	116
7.8 Visualized surfaces of untreated and 5 M HNO ₃ -treated chars.	116
7.9 Distribution of (a) nitrogen and (b) sulfur contents in overall products and (b) nitrogen and (d) sulfur groups in maltenes obtained from using untreated and 5 M HNO ₃ -treated chars.	119
8.1 Schematic of the pyrolysis experiment.	125
8.2 Overview of total ion chromatograms of maltene solution: (a) GCxGC-TOF/MS chromatogram, (b) surface plot (3D) of N-containing hydrocarbon compounds, and (c) contour plot (2D) showing the distribution of all groups of N-containing compounds of all compounds in tire-derived oil.	129

FIGURE	PAGE	
8.3	Classification of nitrogenous compounds in TDO.	130
8.4	Total ion chromatogram of amines in PPAHs with selected ions (U): 30, 91, 93, 105, 106, 117, 148, 150 and 165.	132
8.5	Structures of dominant N-containing compounds in amine group.	133
8.6	Total ion chromatogram of amides in PPAHs with selected ions (U): 66, 93, 147, and 169.	134
8.7	Structures of dominant N-containing compounds in amide group.	135
8.8	Total ion chromatogram of azo compounds in PPAHs with selected ions (U): 96, 108, 119, 132,133, 135, 148, 150, 163, 164, 210, and 211.	136
8.9	Structures of dominant N-containing compounds in azo compound group	136
8.10	Total ion chromatogram of diazabicycloheptenes in PPAHs with selected ions (U): 94, 142, 155, 157, 172, and 220.	138
8.11	Structures of dominant N-containing compounds in diazabicycloheptene group	138
8.12	Total ion chromatogram of indoles in PPAHs with selected ions (U): 118, 130, 132, and 144.	139
8.13	Structures of dominant N-containing compounds in indole group.	139
8.14	Total ion chromatogram of isothiocyanates in PPAHs with selected ions (U): 77, 135, 148, and 149.	140
8.15	Structures of dominant N-containing compounds in isothiocyanate group.	141

FIGURE	PAGE
8.16 Total ion chromatogram of nitro compound in PPAHs with selected ions (U): 91, 97, 105, and 119.	142
8.17 Structures of dominant N-containing compounds in nitro compound group.	143
8.18 Total ion chromatogram of nitriles in PPAHs with selected ions (U): 90, 91, 103, 116, 119, 130, 131, and 159.	144
8.19 Structures of dominant N-containing compounds in nitrile group.	144
8.20 Total ion chromatogram of pyridines in PPAHs with selected ions (U): 106, 117, and 167.	145
8.21 Structures of dominant N-containing compounds in pyridine group.	146
8.22 Total ion chromatogram of pyridines in PPAHs with selected ions (U): 129, 143, 157, 171, and 179.	147
8.23 Structures of dominant N-containing compounds in quinoline group.	147
8.24 Average distribution of N-containing compounds in petroleum fractions.	148
A1 Kinetic diameter of simple and complex compounds.	167
A2 Maximum diameter of simple and complex compounds.	167
A3 Molecular size distributions of components in mono-aromatics (MAHs).	169
A4 Distribution of molecular size of saturated hydrocarbons (SATs).	171
A5 Distribution of molecular size of olefins (OLEs).	172
A6 Distribution of molecular size of naphthenes (NAPs).	173
A7 Distribution of molecular size of terpenes (TERs).	174

FIGURE	PAGE
A8	Distribution of molecular size of mono-aromatics (MAHs). 175
A9	Distribution of molecular size of di-aromatics (DAHs). 176
A10	Distribution of molecular size of poly-aromatics (PAHs). 177
A11	Distribution of molecular size of polar-aromatics (PPAHs). 178
A12	Distribution of large-size molecules ($> 8\text{\AA}$). 179
A13	Distribution of molecular sizes of compounds in tire-derived oil in all petroleum fractions obtain from non-catalyst case: (a) kinetic diameter ($\text{\O}k$) and (b) maximum diameter ($\text{\O}m$). 181
B1	Product distribution. 181
C1	Distribution of gas components. 183
D1	Calibration curve of SIMDIST GC. 185
D2	Boiling point curves obtained from non-catalyst and mesoporous material case 185
D3	Concentration of petroleum fractions in maltenes. 187
D4	Chromatograms obtained from pyrolysis process. 188
D5	Chemical components in maltenes. 190
D6	Petrochemical products in mono-aromatics. 192
E1	Calibration curve of carbon. 197
E2	Calibration curve of hydrogen. 198
E3	Calibration curve of nitrogen. 199
E4	Calibration curve of sulfur. 200
E5	Sulfur distribution in pyrolysis products obtained from waste tire-pyrolysis. 202
E6	Nitrogen distribution in pyrolysis products obtained from waste tire-pyrolysis. 202